LETTERS

Crystal structure of the $\alpha_6\beta_6$ holoenzyme of propionyl-coenzyme A carboxylase

Christine S. Huang[1]*, Kianoush Sadre-Bazzaz[1]*, Yang Shen[1]†, Binbin Deng[2], Z. Hong Zhou[2,3] & Liang Tong[1]

Propionyl-coenzyme A carboxylase (PCC), a mitochondrial biotin-dependent enzyme, is essential for the catabolism of the amino acids Thr, Val, Ile and Met, cholesterol and fatty acids with an odd number of carbon atoms. Deficiencies in PCC activity in humans are linked to the disease propionic acidaemia, an auto-somal recessive disorder that can be fatal in infants[1–4]. The holo-enzyme of PCC is an $\alpha_6\beta_6$ dodecamer, with a molecular mass of 750 kDa. The α-subunit contains the biotin carboxylase (BC) and biotin carboxyl carrier protein (BCCP) domains, whereas the β-subunit supplies the carboxyltransferase (CT) activity. Here we report the crystal structure at 3.2-Å resolution of a bacterial PCC $\alpha_6\beta_6$ holo-enzyme as well as cryo-electron microscopy (cryo-EM) reconstruc-tion at 15-Å resolution demonstrating a similar structure for human PCC. The structure defines the overall architecture of PCC and reveals unexpectedly that the α-subunits are arranged as monomers in the holoenzyme, decorating a central β_6 hexamer. A hitherto unrecognized domain in the α-subunit, formed by resi-dues between the BC and BCCP domains, is crucial for interactions with the β-subunit. We have named it the BT domain. The structure reveals for the first time the relative positions of the BC and CT active sites in the holoenzyme. They are separated by approxi-mately 55 Å, indicating that the entire BCCP domain must trans-locate during catalysis. The BCCP domain is located in the active site of the β-subunit in the current structure, providing insight for its involvement in the CT reaction. The structural informa-tion establishes a molecular basis for understanding the large collection of disease-causing mutations in PCC and is relevant for the holoenzymes of other biotin-dependent carboxylases, including 3-methylcrotonyl-CoA carboxylase (MCC)[5–7] and eukar-yotic acetyl-CoA carboxylase (ACC)[8,9].

PCCs catalyse the carboxylation of propionyl-CoA to produce D-methylmalonyl-CoA. These enzymes are found in organisms from bacteria to humans, with highly conserved amino-acid sequences. For example, the α- and β-subunits of human PCC (HsPCC) and *Ruegeria pomeroyi* PCC (RpPCC) share 54% and 65% sequence iden-tity, respectively (Supplementary Figs 1 and 2). To simplify discus-sions, we have numbered residues in bacterial PCCs according to their equivalents in HsPCC. The BC and BCCP domains in the α-subunit are homologous to their equivalents in ACC and pyruvate carboxylase (PC), whereas the β-subunit is homologous to the CT domain of ACC. The active site of BC is formed by residues from its A and C (sub-)domains, whereas the B (sub-)domain forms a lid that can assume open and closed conformations[9–11]. The active site of CT is located at the interface of its dimer, and each CT contains two (sub-)domains, the N and C domains[9,12]. In contrast to the wealth of information about these domains, little is known about how they are assembled into the holoenzyme of PCC (or ACC).

To prepare samples of the PCC holoenzyme for structural studies, the α- and β-subunits were co-expressed in *Escherichia coli* using a bicistronic plasmid. We first obtained crystals of HsPCC but could not improve the diffraction beyond 5.5 Å resolution after extensive efforts. In addition, the crystals exhibited perfect twinning (space group *R*3). We then examined a collection of bacterial PCCs, and were able to produce crystals of RpPCC that diffracted to 3.3 Å resolution. However, these crystals were also perfectly twinned (space group *P*3). Finally, we discovered that a PCC chimaera, containing the α-subunit of RpPCC and the β-subunit of *Roseobacter denitrificans* PCC (RdPCC), produced crystals without twinning (space group *P*1), and we determined its structure at 3.2 Å resolution (Supplemen-tary Table 1). RdPCC is a close homologue of RpPCC, with their β-subunits sharing 88% sequence identity (Supplementary Fig. 2). The structure of the chimaera is essentially the same as that of the native RpPCC dodecamer (Supplementary Text) as well as that of the HsPCC holoenzyme (see below).

The structure of the $\alpha_6\beta_6$ PCC holoenzyme contains a central β_6 hexamer core, in the shape of a short cylinder with a small hole along its axis (Fig. 1a). This hexameric core can be considered as a trimer of β_2 dimers, with each dimer being formed by one subunit from each layer of the structure (Fig. 1b). In contrast, the α-subunits are arranged as monomers on both ends of the β_6 core, far from the centre of the holoenzyme, with each α-subunit contacting primarily only one β-subunit (see below). There are no significant conforma-tional differences among the six copies of the α- and β-subunits of the holoenzyme (Supplementary Information).

We performed cryo-EM studies on HsPCC and obtained a three-dimensional reconstruction at 15-Å resolution by single-particle ana-lysis (Supplementary Figs 3–6). The cryo-EM envelope is remarkably similar to the overall shape of the crystal structure (Fig. 1c). In fact, the atomic model can be readily fitted into the cryo-EM map, giving a cross-correlation value of 0.80, and only the BCCP domain appears to be in a somewhat different position (Fig. 1d). These studies demonstrate that the structure of HsPCC is highly similar to that of the bacterial enzyme.

An unexpected discovery from the crystal structure of the holo-enzyme is that there is little direct contact between the BC domain in the α-subunit and the β-subunit (Fig. 2a). Instead, interactions with the β-subunit are primarily mediated by a hitherto unrecognized domain in the α-subunit, formed by residues 514–653 in the connec-tion between the BC and BCCP domains (Supplementary Fig. 1). We have named it the BT domain, as it mediates BC–CT interactions. The BT domain has well-defined electron density (Supplementary Fig. 7), suggesting that it is highly ordered in the holoenzyme. A total of $1,950\,\text{Å}^2$ of the surface area of each α-subunit is buried at the interface with the β-subunits. Only $200\,\text{Å}^2$ are contributed by the

[1]Department of Biological Sciences, Columbia University, New York, New York 10027, USA. [2]Department of Pathology and Laboratory Medicine, University of Texas Medical School at Houston, Houston, Texas 77030, USA. [3]Department of Microbiology, Immunology and Molecular Genetics, University of California, Los Angeles, Los Angeles, California 90095, USA. †Present address: Department of Antibody Technology, ImClone Systems, 180 Varick Street, 6th Floor, New York, New York 10014, USA. *These authors contributed equally to this work.
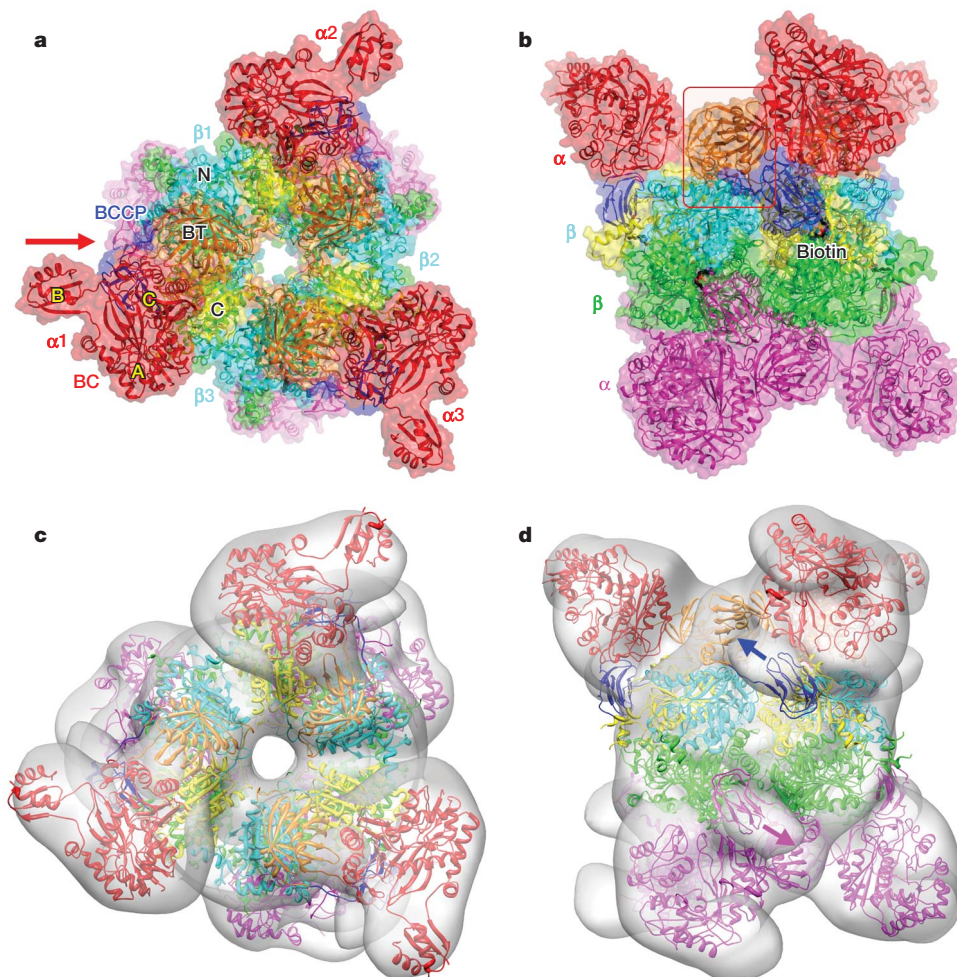
Figure 1 | Structure of the PCC holoenzyme. a, Structure of the RpPCCα–RdPCCβ chimaera, viewed down the threefold symmetry axis. Domains in the α- and β-subunits in the top half of the structure are given different colours, and those in the first α- and β-subunits are labelled. The α- and β-subunits in the bottom half are coloured in magenta and green, respectively. Red arrow, the viewing direction of **b. b,** Structure of the RpPCCα–RdPCCβ chimaera, viewed down the twofold symmetry axis. Red rectangle, the region shown in detail in Fig. 2a. **c,** Cryo-EM reconstruction of HsPCC at 15-Å resolution, viewed in the same orientation as **a.** The atomic model of the chimaera was fit into the cryo-EM envelope. **d,** Cryo-EM reconstruction viewed in the same orientation as **b.** Arrows, a change in the BCCP position that is needed to fit the cryo-EM map. All the structure figures were produced with PyMOL (www.pymol.org), and the cryo-EM figures were produced with Chimera[30].

BC domain (Fig. 2a). In contrast, the BT domain contributes 1,300 Å^2 to the buried surface area with one β-subunit, and an additional 100 Å^2 with an adjacent β-subunit (Fig. 2a). Finally, the BCCP domain contributes 350 Å^2 to the interface (see below).

The BT domain contains a long helix (αV, Supplementary Fig. 1) at the amino (N) terminus, followed by an eight-stranded up–down β-barrel (β22-β29) that surrounds the N-terminal two-thirds of the helix (Fig. 2a and Supplementary Fig. 8). The carboxy (C)-terminal one-third of the helix and the long loop connecting to the first β-strand protrude from the β-barrel, and form a 'hook' that provides a major contact with the β-subunit (Fig. 2b and Supplementary Fig. 8). A second area of close contact with the β-subunit is mediated by a small helix (αW) at the end of the BT domain (Fig. 2c and Supplementary Fig. 8), which projects away from the β-barrel (Fig. 2a). The BT domain does not have any close structural homologues in Protein Data Bank, based on an analysis with the program DaliLite[13]. Remarkably, however, the domain does share some structural similarity with the PC tetramerization (PT) domain, which helps mediate the tetramerization of PC (Supplementary Information and Supplementary Fig. 9)[14].

Many residues are located in the interface between the α- and β-subunits (Supplementary Figs 1 and 2), forming ion-pair, hydrogen-bonding and hydrophobic interactions (Supplementary Information). Residues making important contributions to the interface are generally conserved or show conservative variations among the PCC enzymes (Supplementary Figs 1 and 2), consistent with our observations that HsPCC has a similar structure. Our mutagenesis data confirm the extensive nature of the α–β-subunit interface and suggest that the holoenzyme can withstand substantial disruptions in it (Supplementary Information and Supplementary Table 2).

Another unexpected discovery from the structure is that the BC domains are arranged as monomers in the PCC holoenzyme (Fig. 1a). Studies of the BC subunit of bacterial ACCs have shown a dimeric association[9–11], which may be required for its activity[15], although monomeric BC mutants are catalytically active[16]. A conserved dimeric association of the BC domain was also observed in PC[14,17]. However, the BC domains in PCC are monomeric and, in fact, there are no contacts among the α-subunits in the holoenzyme (Fig. 1a). Our structure defines the molecular basis for the lack of dimerization of the BC domain in PCC (Supplementary Information). A monomeric arrangement of the BC domains also has significant relevance for the holoenzyme of eukaryotic ACCs (see below).

The active site of the BC domain is conserved with that of *E. coli* BC, and all the residues that interact with the substrates of this reaction have essentially the same conformation in both structures (Supplementary Fig. 10)[18]. Similarly, residues in the active site of CT, located at the interface of a β-subunit dimer (Fig. 3a), are also conserved. The structure of this dimer is homologous to those of the
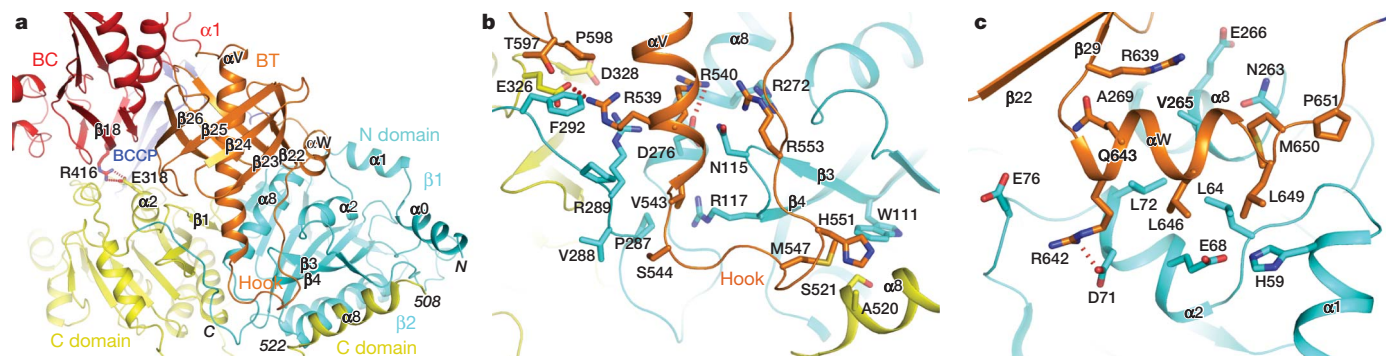
Figure 2 | Interactions between the α- and β-subunits in the PCC holoenzyme. a, Interface between the α- and β-subunits in the RpPCCα–RdPCCβ chimaera. **b**, Detailed interactions between the hook in the BT domain of the α-subunit and the β-subunits. The C-terminal helix

(α8) of an adjacent β-subunit (labelled β2) is also shown. **c**, Detailed interactions between helix αW in the BT domain and the β-subunit. The view is related to that of **a** through a 90° rotation around the vertical axis. See Supplementary Fig. 8 for stereo versions of **b** and **c**.

Streptomyces coelicolor and *Mycobacterium tuberculosis* acyl-CoA carboxylase β-subunits[19,20] and the 12S subunit of *Propionibacterium shermanii* transcarboxylase (Supplementary Fig. 11)[21], which also form similar hexamers. Weaker structural similarity is observed with the CT domain of yeast ACC[12], the CT subunit of bacterial ACC[22] and the CT subunit of a bacterial sodium pump[23], although these CT enzymes only form dimers. A helical sub-domain at the C terminus of the CT domain of yeast ACC is incompatible with the β_6 hexamer of PCC.

Our structure reveals for the first time the relative positions of the BC and CT active sites in the holoenzyme, providing unprecedented insight into PCC catalysis. The distance between the two active sites in PCC is about 55 Å (Fig. 3a); consequently the entire BCCP domain must translocate during catalysis (Supplementary Information and Supplementary Fig. 12). A similar situation has been observed in the structure of PC, where the BC and CT active sites are separated by

75 Å[14,17]. Our cryo-EM studies on HsPCC have provided direct experimental evidence that the BCCP domain can be located in different positions in the holoenzyme (Fig. 1d). Residues 654–660, the linker between the BT and BCCP domains, have weak electron density and are exposed to the solvent in the current structure (Fig. 1b), suggesting that they are flexible and can facilitate the translocation.

Further insight into PCC catalysis is obtained from the binding of the BCCP domain and its associated biotin, with well-defined electron density (Supplementary Fig. 13), in the CT active site (Fig. 3a). The interface between BCCP and the β-subunit is small, with 350-Å² surface area burial. Only residues 693–697 around the biotinylation site (Lys 694) interact with the β-subunit, through hydrophobic interactions and one hydrogen bond (Fig. 3b and Supplementary Fig. 14). This weak interaction should also help the BCCP domain to leave the CT active site and translocate to the BC active site during catalysis.
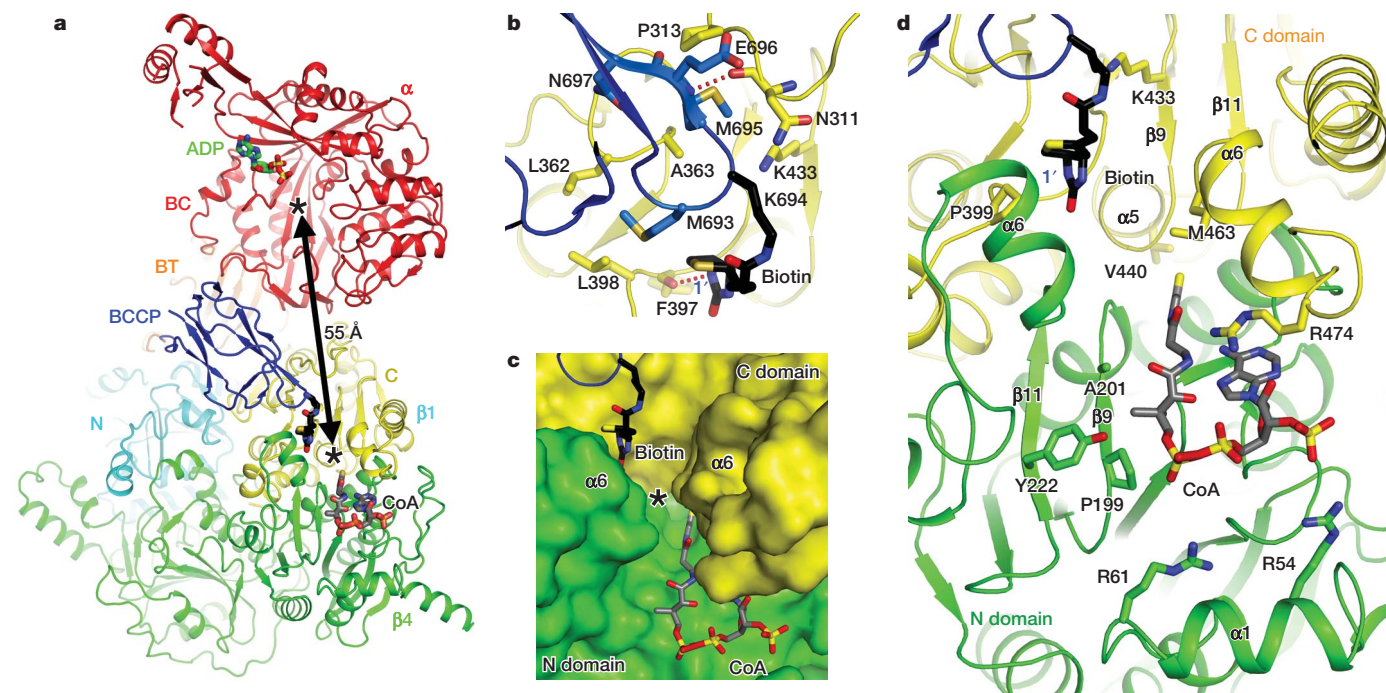

Figure 3 | The active sites of the PCC holoenzyme. a, Relative positioning of the BC and CT active sites in the holoenzyme. One α-subunit and a β₂ dimer (β1 from one layer and β4 from the other layer) are shown, and the viewing direction is the same as Fig. 1b. The two active sites are indicated with the stars, separated by a distance of 55 Å. The bound positions of ADP in complex with *E. coli* BC[18] and that of CoA in complex with the 12S subunit of transcarboxylase[21] are also shown. **b**, Detailed interactions between

BCCP-biotin and the C domain of a β-subunit. Hydrogen-bonding interactions are indicated with the dashed lines in red. The N1′ atom of biotin is labelled as 1′, hydrogen-bonded to the main-chain carbonyl of Phe 397. **c**, Molecular surface of the CT active site, showing a deep canyon where both substrates are bound. **d**, Schematic drawing of the CT active site. See Supplementary Fig. 14 for stereo versions of **b** and **d**.

The active site of CT is located in a deep canyon at the β-subunit dimer interface (Fig. 3c). The α6 helix from the C domain of one subunit and the α6 helix from the N domain of the other subunit form the two walls of the canyon. Our structure shows that BCCP-biotin occupies one half of the canyon, interacting with the C domain of one subunit (Fig. 3d and Supplementary Fig. 14). Propionyl-CoA, the other substrate of this activity, is expected to occupy the other half of the canyon and interact with the N domain of the second β-subunit (Fig. 3d)[12,19,21], with the propionyl group located in the centre of the canyon (Fig. 3c). Biotin is in a partly folded, unproductive conformation in the current structure (Fig. 3b), although a conformational change in the side chain of Lys 694 and the valeryl group of biotin should readily bring the N1′ atom into the proximity of propionyl-CoA for catalysis.

Both RpPCC and the RpPCCα–RdPCCβ chimaera have a preference for propionyl-CoA over acetyl-CoA as the substrate (Supplementary Table 4). Earlier studies with *Streptomyces coelicolor* acyl-CoA carboxylase showed that residue Asp 422—equivalent to Asp 440 in HsPCC and RpPCC and Val 440 in RdPCC (in helix α5, Fig. 3d)—is important for discriminating between the two substrates[19]. However, equivalent mutations in PCCs—D440I for RpPCC and V440I for the RpPCCα–RdPCCβ chimaera—did not change their substrate preference (Supplementary Table 4). Residue 440 is about 10 Å away from the thiol group of CoA (Fig. 3d) and does not directly contribute to substrate binding. Other residues may also be improtant in determining the substrate preference of these enzymes.

The structure of the holoenzyme establishes a foundation for understanding the molecular basis of many disease-causing mutations in PCC (Fig. 4 and Supplementary Table 3)[1–4]. Among these, only the R399Q mutation in the α-subunit directly disrupts a residue in the active site (Supplementary Fig. 15). This side chain stabilizes the biotin enolate during BC catalysis (Supplementary Fig. 10)[18], and the mutation leads to a large loss in activity[18,24]. Another mutation, G668R in the BCCP domain (Fig. 4), abolishes biotinylation. Many of the other mutations are detrimental to catalysis by destabilizing the enzyme and/or interfering with holoenzyme assembly[1,25–27]. Many of them, especially those in the β-subunit, are actually located near the active site (Supplementary Fig. 15), and they may indirectly affect substrate binding and/or catalysis as well. For example, the R165W

and R165Q mutations may disturb the recognition of the adenine base of CoA (Supplementary Fig. 15). On the other hand, few of the missense mutations are located in the interface between the α- and β-subunits of the holoenzyme (Fig. 4 and Supplementary 16). The extensive nature of this interface might make it difficult to disrupt the holoenzyme by single-site mutations in this region (Supplementary Information).

The structure of the PCC holoenzyme also has strong implications for the structure and function of other biotin-dependent carboxylases. There are five such enzymes in humans: PCC, MCC, ACC1, ACC2 and PC (Supplementary Fig. 17). MCC is a close homologue of PCC, with the same domain architecture and subunit organization. Therefore the PCC structure is directly relevant for understanding the MCC enzyme and its disease-causing mutations[5–7].

Most importantly, the identification of the BT domain in PCC led us to re-examine the sequences of eukaryotic, multi-domain ACCs. The segment containing the BC and BCCP domains in these enzymes is remarkably similar to the PCC α-subunit, with a linker of about 120 residues between the two domains (Supplementary Fig. 17). Secondary structure prediction shows that this linker contains a helix followed by seven or more β-strands, suggesting that it may form a structure similar to the BT domain in PCC. This putative BT domain of ACC is likely also crucial for mediating interactions between its BC and CT domains. In fact, we have observed that purified BC and CT domains of yeast ACC do not interact with each other (unpublished results). Because the CT domain dimer of ACC is similar to the β2 dimer of PCC, the α2β2 assembly of PCC might be a plausible model for the organization of the ACC dimer, the protomer that can also form higher oligomers. This model implies that the BC domain could be monomeric in the ACC holoenzyme, which is consistent with observations that isolated BC domains of eukaryotic ACCs are monomeric in solution[28,29], in contrast to the dimers for bacterial BC subunits. Therefore, there might be a fundamental difference between the overall architecture of eukaryotic, multi-domain ACCs and that of bacterial, multi-subunit ACCs.

METHODS SUMMARY

Crystallography. The α- and β-subunits of PCC were co-expressed in *E. coli*, with a His-tag on the β-subunit. The PCC holoenzyme was purified by nickel-affinity and gel-filtration chromatography. Crystals were obtained by the micro-batch method under oil, and the structures were determined by the molecular replacement method.

Cryo-EM. Frozen hydrated human PCC particles at 70 μg ml^{-1} concentration were imaged at ×50,000 magnification in a 100-kV cryo-electron microscope. A featureless Gaussian oval was used to obtain a low-resolution (40-Å) model from negative-stain electron microscope images. A 15-Å resolution three-dimensional reconstruction was obtained from approximately 10,000 cryo-EM particle images, using the structure from the negative stain images as the initial model.

Mutagenesis and kinetic studies. Site-specific and deletion mutants were designed based on the structural information, and their effects on the formation of the holoenzyme were assessed by nickel-affinity chromatography. The catalytic activity of PCC was determined by a coupled enzyme assay, monitoring the hydrolysis of ATP.

Full Methods and any associated references are available in the online version of the paper at www.nature.com/nature.
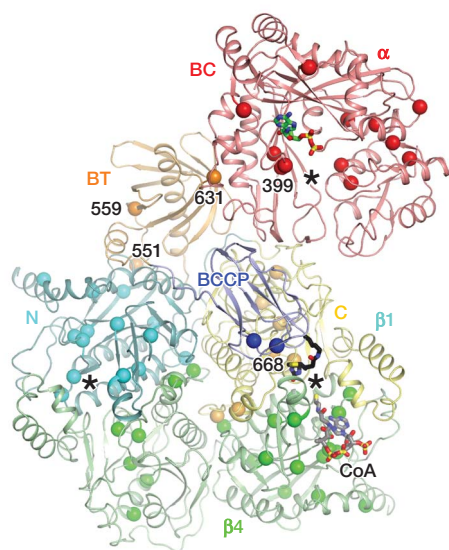
Figure 4 | Locations of disease-causing mutations in the PCC holoenzyme. Structure of one α-subunit and one β2-subunit dimer of PCC, in the same view as Fig. 3a. The locations of the missense mutations associated with propionic acidaemia are indicated with the spheres, coloured by the domains. The BC and CT active sites are indicated with the stars.

1. Desviat, L. R. et al. Propionic acidemia: mutation update and functional and structural effects of the variant alleles. Mol. Genet. Metab. 83, 28–37 (2004).
2. Rodriguez-Pombo, P. et al. Towards a model to explain the intragenic complementation in the heteromultimeric protein propionyl-CoA carboxylase. Biochim. Biophys. Acta 1740, 489–498 (2005).
3. Deodato, F., Boenzi, S., Santorelli, F. M. & Dionisi-Vici, C. Methylmalonic and propionic aciduria. Am. J. Med. Genet. C. Semin. Med. Genet. 142, 104–112 (2006).
4. Desviat, L. R. et al. New splicing mutations in propionic acidemia. J. Hum. Genet. 51, 992–997 (2006).
5. Desviat, L. R. et al. Functional analysis of MCCA and MCCB mutations causing methylcrotonylglycinuria. Mol. Genet. Metab. 80, 315–320 (2003).
6. Stadler, S. C. et al. Newborn screening for 3-methylcrotonyl-CoA carboxylase deficiency: population heterogeneity of MCCA and MCCB mutations and impact on risk assessment. Hum. Mutat. 27, 748–759 (2006).

7. Stucki, M., Suormala, T., Fowler, B., Valle, D. & Baumgartner, M. R. Cryptic exon activation by disruption of exon splice enhancer. Novel mechanism causing 3-methylcrotonyl-CoA carboxylase deficiency. *J. Biol. Chem.* **284**, 28953–28957 (2009).
8. Wakil, S. J., Stoops, J. K. & Joshi, V. C. Fatty acid synthesis and its regulation. *Annu. Rev. Biochem.* **52**, 537–579 (1983).
9. Tong, L. Acetyl-coenzyme A carboxylase: crucial metabolic enzyme and attractive target for drug discovery. *Cell. Mol. Life Sci.* **62**, 1784–1803 (2005).
10. Waldrop, G. L., Rayment, I. & Holden, H. M. Three-dimensional structure of the biotin carboxylase subunit of acetyl-CoA carboxylase. *Biochem.* **33**, 10249–10256 (1994).
11. Cronan, J. E. Jr & Waldrop, G. L. Multi-subunit acetyl-CoA carboxylases. *Prog. Lipid Res.* **41**, 407–435 (2002).
12. Zhang, H., Yang, Z., Shen, Y. & Tong, L. Crystal structure of the carboxyltransferase domain of acetyl-coenzyme A carboxylase. *Science* **299**, 2064–2067 (2003).
13. Holm, L., Kaariainen, S., Rosenstrom, P. & Schenkel, A. Searching protein structure databases with DaliLite v.3. *Bioinformatics* **24**, 2780–2781 (2008).
14. Xiang, S. & Tong, L. Crystal structures of human and *Staphylococcus aureus* pyruvate carboxylase and molecular insights into the carboxyltransfer reaction. *Nature Struct. Mol. Biol.* **15**, 295–302 (2008).
15. Janiyani, K., Bordelon, T., Waldrop, G. L. & Cronan, J. E. Jr. Function of *Escherichia coli* biotin carboxylase requires catalytic activity of both subunits of the homodimer. *J. Biol. Chem.* **276**, 29864–29870 (2001).
16. Shen, Y., Chou, C.-Y., Chang, G.-G. & Tong, L. Is dimerization required for the catalytic activity of bacterial biotin carboxylase? *Mol. Cell* **22**, 807–818 (2006).
17. St. Maurice, M. *et al.* Domain architecture of pyruvate carboxylase, a biotin-dependent multifunctional enzyme. *Science* **317**, 1076–1079 (2007).
18. Chou, C.-Y., Yu, L. P. C. & Tong, L. Crystal structure of biotin carboxylase in complex with substrates and implications for its catalytic mechanism. *J. Biol. Chem.* **284**, 11690–11697 (2009).
19. Diacovich, L. *et al.* Crystal structure of the b-subunit of acyl-CoA carboxylase: structure-based engineering of substrate specificity. *Biochem.* **43**, 14027–14036 (2004).
20. Lin, T. W. *et al.* Structure-based inhibitor design of AccD5, an essential acyl-CoA carboxylase carboxyltransferase domain of Mycobacterium tuberculosis. *Proc. Natl Acad. Sci. USA* **103**, 3072–3077 (2006).
21. Hall, P. R. *et al.* Transcarboxylase 12S crystal structure: hexamer assembly and substrate binding to a multienzyme core. *EMBO J.* **22**, 2334–2347 (2003).
22. Bilder, P. *et al.* The structure of the carboxyltransferase component of acetyl-CoA carboxylase reveals a zinc-binding motif unique to the bacterial enzyme. *Biochem.* **45**, 1712–1722 (2006).
23. Wendt, K. S., Schall, I., Huber, R., Buckel, W. & Jacob, U. Crystal structure of the carboxyltransferase subunit of the bacterial sodium ion pump glutaconyl-coenzyme A decarboxylase. *EMBO J.* **22**, 3493–3502 (2003).
24. Sloane, V. & Waldrop, G. L. Kinetic characterization of mutations found in propionic acidemia and methylcrotonylglycinuria. *J. Biol. Chem.* **279**, 15772–15778 (2004).
25. Jiang, H., Rao, K. S., Yee, V. C. & Kraus, J. P. Characterization of four variant forms of human propionyl-CoA carboxylase expressed in *Escherichia coli. J. Biol. Chem.* **280**, 27719–27727 (2005).
26. Muro, S. *et al.* Effect of PCCB gene mutations on the heteromeric and homomeric assembly of propionyl-CoA carboxylase. *Mol. Genet. Metab.* **74**, 476–483 (2001).
27. Perez-Cerda, C. *et al.* Functional analysis of PCCB mutations causing propionic acidemia based on expression studies in deficient human skin fibroblasts. *Biochim. Biophys. Acta* **1638**, 43–49 (2003).
28. Shen, Y., Volrath, S. L., Weatherly, S. C., Elich, T. D. & Tong, L. A mechanism for the potent inhibition of eukaryotic acetyl-coenzyme A carboxylase by soraphen A, a macrocyclic polyketide natural product. *Mol. Cell* **16**, 881–891 (2004).
29. Weatherly, S. C., Volrath, S. L. & Elich, T. D. Expression and characterization of recombinant fungal acetyl-CoA carboxylase and isolation of a soraphen-binding domain. *Biochem. J.* **380**, 105–110 (2004).
30. Pettersen, E. F. *et al.* UCSF Chimera – a visualization system for exploratory research and analysis. *J. Comput. Chem.* **25**, 1605–1612 (2004).

Author Contributions C.S.H., K.S.-B., Y.S. and B.D. performed the experiments, analysed the data and commented on the manuscript. L.T. and Z.H.Z. designed and performed the experiments, analysed the data and wrote the manuscript.

Author Information The atomic coordinates are deposited in Protein Data Bank under accession number 3N6R. Reprints and permissions information is available at www.nature.com/reprints. The authors declare no competing financial interests. Readers are welcome to comment on the online version of this article at www.nature.com/nature. Correspondence and requests for materials should be addressed to L.T. (ltong@columbia.edu).

METHODS

Protein expression and purification. The α-subunit of PCC was amplified by PCR from genomic DNA and inserted into the pET-26b vector (Novagen) using the restriction enzymes NdeI and NotI (New England Biolabs). The β-subunit was cloned into pET-28a using NdeI and EcoRI, introducing an N-terminal hexahistidine tag. The PCCα insert in pET-26b, together with the upstream ribosomal binding site, was then placed to the 3′-end of the PCCβ insert to make a bicistronic expression plasmid. The plasmid was transformed into *E. coli* BL21Star (DE3) cells (Invitrogen). Biotin at $20\,mg\,l^{-1}$ concentration was supplemented into the growth media. After induction with 1 mM IPTG, the cells were allowed to grow overnight at 25 °C. Cells were lysed by sonication in a buffer containing 20 mM Tris (pH 7.4), 250 mM NaCl, 5% (v/v) glycerol, 0.1% (v/v) Triton X-100 and 10 mM β-mercaptoethanol. Soluble PCC was purified by Ni-NTA (Qiagen) and gel filtration (Sephacryl S-300, GE Healthcare) chromatography. Purified protein was concentrated to $15\,mg\,ml^{-1}$ in a buffer containing 25 mM Tris (pH 7.4), 250 mM NaCl, 2 mM DTT and 5% (v/v) glycerol, flash-frozen in liquid nitrogen and stored at −80 °C. The N-terminal His-tag on PCC-β was not removed for crystallization. Complete biotinylation of the α-subunit was confirmed by an avidin gel-shift assay.

Protein crystallization. Crystals of the RpPCCα–RdPCCβ chimaera were obtained at 4 °C using the microbatch method under paraffin oil. The protein was at $15\,mg\,ml^{-1}$ concentration, and the precipitant solution contained 0.1 M HEPES (pH 8.0), 22% (w/v) PEG3350, 0.2 M NaCl and 16% (v/v) glycerol. Most of these crystals diffracted X-rays poorly and were highly mosaic. A few of good quality were identified after screening through many of them.

Crystals of RpPCC were obtained at 20 °C using the microbatch method under paraffin oil. The protein was at $15\,mg\,ml^{-1}$ concentration, and the precipitant solution contained 0.2 M succinic acid (pH 6.5), 22% (w/v) benzamidine and 22% (w/v) PEG3000. The diffraction quality of most of these crystals was also very poor.

Crystals of HsPCC were obtained at 4 °C using the sitting-drop vapour-diffusion method. The protein was at $15\,mg\,ml^{-1}$ concentration, and the precipitant solution contained 0.1 M Tris (pH 8.5), 5% (w/v) PEG8000, 13% (v/v) PEG300 and 8% (v/v) glycerol.

Data collection and structure determination. An X-ray diffraction data set to 3.2-Å resolution on the RpPCC-α–RdPCC-β chimaera was collected at the X29A beamline of the National Synchrotron Light Source. The crystal belonged to space group *P*1, with cell parameters of *a* = 133.9 Å, *b* = 159.2 Å, *c* = 153.7 Å, α = 113.9°, β = 101.0° and γ = 109.0°. There is one $\alpha_6\beta_6$ dodecamer in the asymmetric unit/unit cell. The diffraction data were processed and scaled with the HKL package[31]. The structure was solved by the molecular replacement method with the program Phaser[32]. The structures of the BC subunit of *E. coli* ACC[33], the β-subunit of *S. coelicolor* acyl-CoA carboxylase[34] and the BCCP domain of *Staphylococcus aureus* PC[35] were used as search models. Sixfold non-crystallographic symmetry averaging was performed with the program DM in the CCP4 package[36]. The atomic model was built into the electron density map with the program O[37]. The structure refinement was performed with the program CNS[38]. Non-crystallographic symmetry restraints were used during the refinement. The data processing and refinement statistics are summarized in Supplementary Table 1.

An X-ray diffraction data set to 3.2-Å resolution on RpPCC was collected at the X29A beamline of the National Synchrotron Light Source. The crystal belonged to space group *P*3, with cell parameters of *a* = *b* = 246.3 Å and *c* = 133.5 Å. There are three $\alpha_2\beta_2$ assemblies in the asymmetric unit, situated at the crystallographic threefold axis. The crystal exhibited perfect merohedral twinning, with a twinning fraction of 0.49. The structure was solved by the molecular replacement method with the program COMO[39], using the structure of the PCC chimaera as the search model. Twinned structure refinement was performed with the program CNS.

An X-ray diffraction data set to 5.5-Å resolution on HsPCC was collected at the X4A beamline of the National Synchrotron Light Source. The crystal belonged to space group *R*3, with cell parameters of *a* = *b* = 196.1 Å and *c* = 979.5 Å. The crystal also exhibited perfect merohedral twinning, and attempts to solve this structure have been unsuccessful.

Electron microscopy. Highly purified HsPCC sample was diluted to $70\,\mu g\,ml^{-1}$ with 1 × PBS buffer (pH 7.4). For negative stain electron microscopy, an aliquot of 3-μl sample was placed onto a carbon-film-coated, glow-discharged, 300-mesh copper grid. Excess sample was blotted away after 1 minute. The sample was stained twice with 2.5% uranyl acetate solution and air dried. For cryo-EM, frozen hydrated HsPCC particles were suspended across holes of Quantifoil holey carbon grids by plunge-freezing immediately after dilution following standard procedures. Cryo-EM was performed using a JEOL 1200EX electron microscope. Electron micrographs were recorded on Kodak SO163 films at ×50,000 magnification and digitized using a Zeiss SCAI scanner with a step size of 14 μm per pixel, corresponding to 2.8 Å per pixel on the sample (Supplementary Fig. 4).

Single particle analysis was performed using the EMAN software package[40]. To eliminate possible model bias, a featureless elliptical Gaussian ball was used as a starting model to process the high-contrast negative-stain images to obtain a low-resolution structure of HsPCC (Supplementary Fig. 5). This low-resolution reconstruction exhibited features consistent with D3 symmetry, in agreement with the expected symmetry of the β_6 core of PCC[34]. Subsequently, D3 symmetry was imposed on the three-dimensional model obtained from the negative stain images.

For the cryo-EM reconstruction, approximately 15,000 particles were picked from digitized micrographs semi-automatically using the boxer program in EMAN. The three-dimensional reconstruction from the negative-stain images was low-pass filtered to 40-Å resolution and used as the starting model for processing the cryo-EM images. Particle images were classified and class averages generated (Supplementary Fig. 6). D3 symmetry was imposed during refinement and three-dimensional reconstruction. The resolution of the three-dimensional reconstruction was assessed by monitoring the Fourier shell correlation between three-dimensional reconstructions from the two half sets of the whole data set (Supplementary Fig. 7). The structure was refined iteratively until no further improvement in the resolution of the reconstruction could be obtained. Approximately 10,000 particles were used in the final three-dimensional reconstruction (Supplementary Fig. 7). The University of California, San Francisco (UCSF) Chimera program was used to create three-dimensional graphical representations[41]. The atomic model of PCC was first manually fitted into the cryo-EM density map, and the fitting was refined using the fit-model-to-map module of Chimera.

Mutagenesis and kinetic studies. Site-specific mutations were introduced in RpPCC with the QuikChange Kit (Stratagene) and sequenced for confirmation. Deletion mutations were created by introducing a stop codon through mutagenesis at the desired position in RpPCC. The mutant plasmids were transformed into *E. coli*, and the formation of the holoenzyme was assessed by nickel-affinity chromatography.

The catalytic activity of PCC was determined using a coupled enzyme assay, converting the hydrolysis of ATP to the disappearance of NADH[34,42]. The reaction mixture contained 100 mM HEPES (pH 8.0), 0.5 mM ATP, 8 mM $MgCl_2$, 40 mM $KHCO_3$, 0.5 mM propionyl-CoA or acetyl-CoA, 0.2 mM NADH, 0.5 mM phosphoenolpyruvate, 7 units of lactate dehydrogenase, 4.2 units of pyruvate kinase and 200 mM KCl. The absorbance at 340 nm was monitored for 5 min.

31. Otwinowski, Z. & Minor, W. Processing of X-ray diffraction data collected in oscillation mode. *Methods Enzymol.* **276**, 307–326 (1997).
32. McCoy, A. J. *et al.* Phaser crystallographic software. *J. Appl. Cryst.* **40**, 658–674 (2007).
33. Thoden, J. B., Blanchard, C. Z., Holden, H. M. & Waldrop, G. L. Movement of the biotin carboxylase B-domain as a result of ATP binding. *J. Biol. Chem.* **275**, 16183–16190 (2000).
34. Diacovich, L. *et al.* Crystal structure of the β-subunit of acyl-CoA carboxylase: structure-based engineering of substrate specificity. *Biochemistry* **43**, 14027–14036 (2004).
35. Xiang, S. & Tong, L. Crystal structures of human and *Staphylococcus aureus* pyruvate carboxylase and molecular insights into the carboxyltransfer reaction. *Nature Struct. Mol. Biol.* **15**, 295–302 (2008).
36. CCP4. The CCP4 suite: programs for protein crystallography. *Acta Crystallogr. D* **50**, 760–763 (1994).
37. Jones, T. A., Zou, J. Y., Cowan, S. W. & Kjeldgaard, M. Improved methods for building protein models in electron density maps and the location of errors in these models. *Acta Crystallogr. A* **47**, 110–119 (1991).
38. Brunger, A. T. *et al.* Crystallography & NMR System: a new software suite for macromolecular structure determination. *Acta Crystallogr. D* **54**, 905–921 (1998).
39. Jogl, G., Tao, X., Xu, Y. & Tong, L. COMO: a program for combined molecular replacement. *Acta Crystallogr. D* **57**, 1127–1134 (2001).
40. Ludtke, S. J., Baldwin, P. R. & Chiu, W. EMAN: semiautomated software for high-resolution single-particle reconstructions. *J. Struct. Biol.* **128**, 82–97 (1999).
41. Pettersen, E. F. *et al.* UCSF Chimera – a visualization system for exploratory research and analysis. *J. Comput. Chem.* **25**, 1605–1612 (2004).
42. Blanchard, C. Z., Lee, Y. M., Frantom, P. A. & Waldrop, G. L. Mutations at four active site residues of biotin carboxylase abolish substrate-induced synergism by biotin. *Biochemistry* **38**, 3393–3400 (1999).